



# Structural and optical emission characteristics of InGaN thin layers and the implications for growing high-quality quantum wells by MOCVD

J.T. Kobayashi\*, N.P. Kobayashi, X. Zhang, P.D. Dapkus, D.H. Rich

*Department of Materials Science and Electrical Engineering/Electrophysics, University of Southern California, Los Angeles, CA 90089-0483, USA*

---

## Abstract

Defect formation and In segregation in InGaN/GaN quantum wells grown at various temperatures and with various well thicknesses were studied using cathodoluminescence, transmission electron microscopy (TEM) and high-resolution transmission electron microscopy (HR-TEM).  $\text{In}_{0.16}\text{Ga}_{0.84}\text{N}$  quantum wells with In compositional nonuniformity and a small number of structural defects originating at the InGaN/GaN interface showed sharp and intense InGaN emission in cathodoluminescence (CL). Increasing the In composition caused surface roughness in the InGaN layer and the formation of stacking faults/dislocations originating at InGaN/GaN interface. This resulted in a reduction of the InGaN emission peak intensity. © 1998 Elsevier Science B.V. All rights reserved.

*PACS:* 61.16.Bg; 61.72.Ff; 61.72.Nn; 68.35.Ct; 68.35.Dv; 68.55.Jk; 68.55.Ln; 68.55.Nq; 78.60.Hk; 78.66.Fd; 81.05.Ea; 81.15.Gh

*Keywords:* GaN; InGaN; Quantum well; Metalorganic chemical vapor deposition (MOCVD); AFM; CL; TEM

---

## 1. Introduction

Blue light-emitting devices using InGaN/GaN quantum wells (QWs) have been demonstrated by several researchers [1,2]. Optical properties of InGaN/GaN QWs are very sensitive to the growth conditions of the InGaN layer. The effect of the InGaN layer thickness [3–5], InGaN layer

composition [6], and the InGaN/GaN interface [3,5] on the optical properties have been reported.

Recently, Kawakami et al. reported a study of In segregation in InGaN layers in InGaN/GaN multi-QWs using transmission electron microscopy (TEM) and energy-dispersive X-ray spectroscopy (EDX) [7]. The influence of In segregation on the optical properties also has been reported by several researchers [8–10].

To understand in better detail the correlation between the growth conditions and the optical

---

\*Corresponding author. E-mail: kobayash@scf.usc.edu.

properties and to find a way to control the In segregation, we have studied structural defect formation and In segregation in InGaN/GaN QWs grown at various temperatures and to various thicknesses using cathodoluminescence, TEM and high-resolution transmission electron microscopy (HR-TEM). In this paper, we show how the growth conditions affect the formation of structural defects and In segregation. We also discuss how the optical properties of InGaN are influenced by structural defects and In segregation.

## 2. Experimental procedure

InGaN/GaN thin heterostructures and QWs were grown on *c*-plane sapphire substrate by atmospheric pressure metalorganic chemical vapor deposition (MOCVD) using a close spaced showerhead reactor. This reactor design utilizes a water-cooled multi-inlet gas distribution showerhead in which the group III and V sources are separately inlet directly ( $\sim 1$  cm) above the substrate. Trimethylgallium (TMGa), trimethylindium (TMI) and  $\text{NH}_3$  were used as precursors. Thin heterostructure samples consist of a 4  $\mu\text{m}$  thick GaN buffer followed by nominal 10–100  $\text{\AA}$  thick InGaN. QW samples consist of 4  $\mu\text{m}$  thick GaN buffer followed by nominal 40–100  $\text{\AA}$  thick InGaN capped with 700  $\text{\AA}$  GaN. For both thin heterostructures and QWs, following the growth of the 4  $\mu\text{m}$  thick GaN via multi-buffer layer approach and multi-overlayer approach [11,12], the growth temperature was decreased rather slowly from 950°C to 800°C with ramp rate of  $-5^\circ\text{C}/\text{min}$  to avoid the formation of pit-shaped defects in InGaN and GaN cap layer [13]. At the same time the carrier gas was switched from  $\text{H}_2$  to  $\text{N}_2$  to enhance In incorporation [4]. For the QW samples, a GaN cap layer was grown without growth interruption after InGaN growth. The growth temperature was changed from 800°C to 950°C during the growth of the GaN cap layer. InGaN layer growth temperatures were 750°C and 775°C, with corresponding In compositions, measured by four crystal X-ray diffractometry, to be 16% and 19%, respectively.

Surface morphology of the thin InGaN film was studied by contact-mode atomic force microscopy

(AFM). Structural defect formation and In segregation were studied by TEM (120 keV) and HR-TEM (200 keV). Optical properties of the QW were studied by cathodoluminescence (CL) with an acceleration voltage of 15 keV at 87 K.

## 3. Results and discussion

Fig. 1 shows AFM images taken on the surface of InGaN single layers grown on GaN with various InGaN growth temperatures and thicknesses. For a sample grown at 750°C, the  $\text{In}_{0.19}\text{Ga}_{0.81}\text{N}$  layer shows corrugation after 50 s growth (nominal thickness of 50  $\text{\AA}$ ) as shown in Fig. 1a. In Fig. 1b, the growth mode of InGaN is shown to change to three-dimensional growth and the surface roughness becomes significant after 100 s growth (nominal thickness of 100  $\text{\AA}$ ). As shown in Fig. 1c and d,  $\text{In}_{0.16}\text{Ga}_{0.84}\text{N}$  layers grown at 775°C shows smoother surfaces compared to  $\text{In}_{0.19}\text{Ga}_{0.81}\text{N}$  layer grown at 750°C, this is likely to be due to the reduction of In composition from 19% to 16% which leads the reduction of misfit strain between InGaN and GaN. For the sample grown at 775°C, after 50 s growth (nominal thickness of 40  $\text{\AA}$ ), the surface is as smooth as the starting GaN surface as shown in Fig. 1c, and even after 100 s growth (nominal thickness of 80  $\text{\AA}$ ), the surface shows only slight roughness as shown in Fig. 1d.

Fig. 2 shows cross-sectional TEM images (Fig. 2a and c) and HR-TEM images (Fig. 2b and d) of  $\text{In}_{0.19}\text{Ga}_{0.81}\text{N}$  QWs grown at 750°C with various well thicknesses. The  $\text{In}_{0.19}\text{Ga}_{0.81}\text{N}$  QW with well thickness of 50  $\text{\AA}$  ( $\text{In}_{\text{high}}$  QW ( $d_w = 50 \text{\AA}$ )) shows many stacking faults associated with dislocations, which originate at the InGaN/GaN interface as seen in Fig. 2a. In the HR-TEM image of the QW, nonuniform strain contrast is observed along both the top and bottom InGaN/GaN interfaces as shown in Fig. 2b. Nonuniformity of misfit strain, probably associated with nonuniformity of In composition in InGaN, at the InGaN/GaN interfaces may cause the observed nonuniform contrast along the interfaces.

The  $\text{In}_{0.19}\text{Ga}_{0.81}\text{N}$  QW with a well thickness of 100  $\text{\AA}$  ( $\text{In}_{\text{high}}$  QW ( $d_w = 100 \text{\AA}$ )) has densely formed dislocations and pit-shaped defects in GaN cap

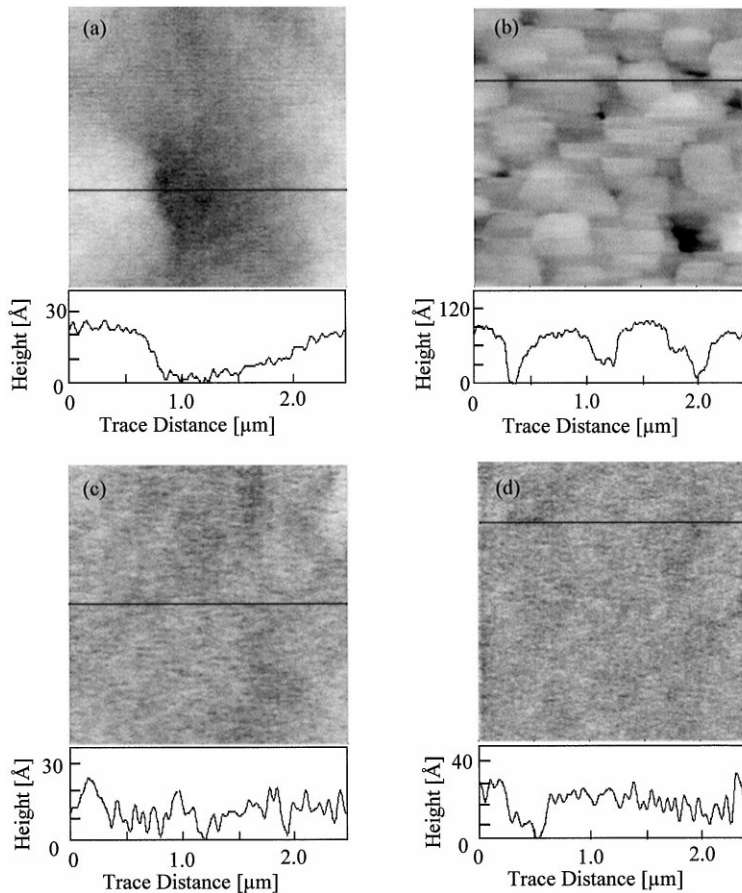


Fig. 1. Contact mode AFM images taken on InGaN single layers grown with various growth temperatures and thicknesses: (a) 750°C for 50 s, (b) 750°C for 100 s, (c) 775°C for 50 s and (d) 775°C for 100 s. A line profile along a solid line in each image is also shown.

layer as shown in Fig. 2c. There is a correlation between the location of pit-shaped defect and the densely dislocated area. The 100 Å  $\text{In}_{0.19}\text{Ga}_{0.81}\text{N}$  thin heterostructure shows a significantly rougher InGaN surface (Fig. 1b) than the other samples. If there is no significant change in surface morphology on InGaN during the sample cool-down after growth, the roughness of InGaN layer before the GaN cap layer growth might cause the growth of a heavily dislocated cap layer with pit shape defects. The HR-TEM image of the QW (Fig. 2d) shows that the InGaN layer is also heavily dislocated.

Fig. 3 shows cross-sectional TEM and HR-TEM images of the  $\text{In}_{0.16}\text{Ga}_{0.84}\text{N}$  QW grown at 775°C with various well thicknesses. Fig. 3a shows TEM

and HR-TEM images of the  $\text{In}_{0.16}\text{Ga}_{0.84}\text{N}$  QW with well thickness of 40 Å ( $\text{In}_{\text{low}}$  QW ( $d_w = 40$  Å)). Within the area of TEM observation (several  $\mu\text{m}$ ), no structural defect originated at the InGaN/GaN interfaces is observed. Since the 40 Å  $\text{In}_{0.16}\text{Ga}_{0.84}\text{N}$  single layer on GaN shows a smooth surface (Fig. 1c), we believe that there is a correlation between InGaN surface roughness and defect formation at InGaN/GaN interface. Inset shows HR-TEM images of the QW. The image shows nonuniform contrast along the InGaN/GaN interfaces, which might be evidence of In compositional nonuniformity as mentioned above.

The  $\text{In}_{0.16}\text{Ga}_{0.84}\text{N}$  QW with well thickness of 80 Å ( $\text{In}_{\text{low}}$  QW ( $d_w = 80$  Å)) shows some stacking

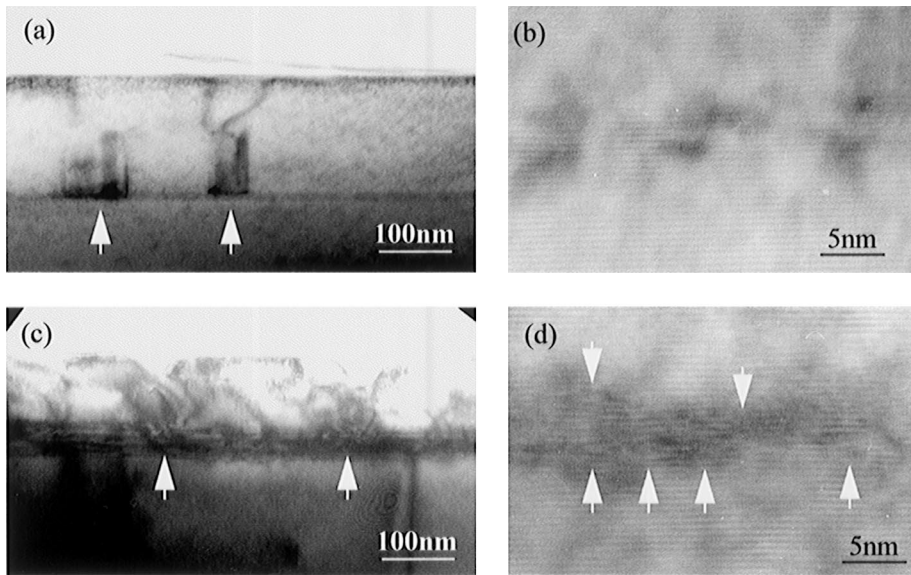


Fig. 2. Cross-sectional, (a) and (c), and high resolution, (b) and (d), TEM images of InGaN/GaN QW. (a) and (b) represent In<sub>high</sub> QW ( $d_w = 50 \text{ \AA}$ ) and (c) and (d) represent In<sub>high</sub> QW ( $d_w = 100 \text{ \AA}$ ). Arrows point structural defects.

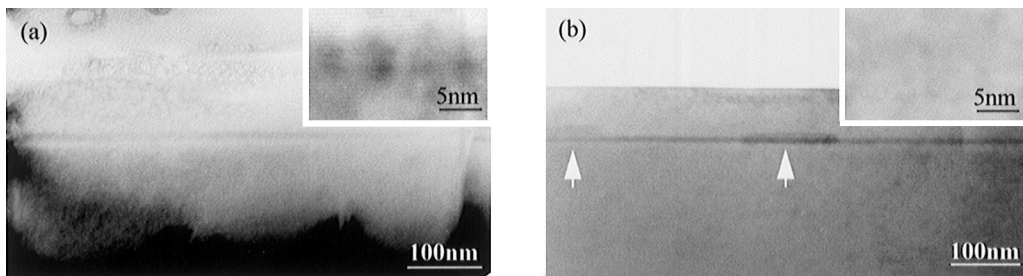


Fig. 3. Cross-sectional TEM images of (a) In<sub>low</sub> QW ( $d_w = 40 \text{ \AA}$ ) and (b) In<sub>low</sub> QW ( $d_w = 80 \text{ \AA}$ ). Insets are HR-TEM images. Arrows indicate structural defects.

faults originated at the InGaN/GaN interface as shown in Fig. 3b, but the density of the defects (stacking faults and dislocations) is much lower compared to QW with higher In content (Fig. 2a and c). We believe the lower In composition suppresses the surface roughness on the InGaN layer. Inset of Fig. 3b shows HR-TEM image of the QW. The image shows a defect-free quantum well layer without any contrast nonuniformity along the InGaN/GaN top interface. Along InGaN/GaN bottom interface, slight contrast difference is observed,

but not as great as seen in the In<sub>high</sub> QW ( $d_w = 50 \text{ \AA}$ ) and the In<sub>low</sub> QW ( $d_w = 40 \text{ \AA}$ ).

Fig. 4 shows CL spectrum taken for the four kinds of QW samples with various thicknesses and In compositions. The In<sub>low</sub> QW ( $d_w = 40 \text{ \AA}$ ) shows strong InGaN emission peak at 406 nm with FWHM of 50 meV (Fig. 4c). No InGaN emission peak was observed for In<sub>high</sub> QW ( $d_w = 100 \text{ \AA}$ ) as shown in Fig. 4b. This might be because of the structural defects created in In<sub>0.19</sub>Ga<sub>0.81</sub>N layer and at InGaN/GaN interfaces as shown in Fig. 2c and Fig. 2d.

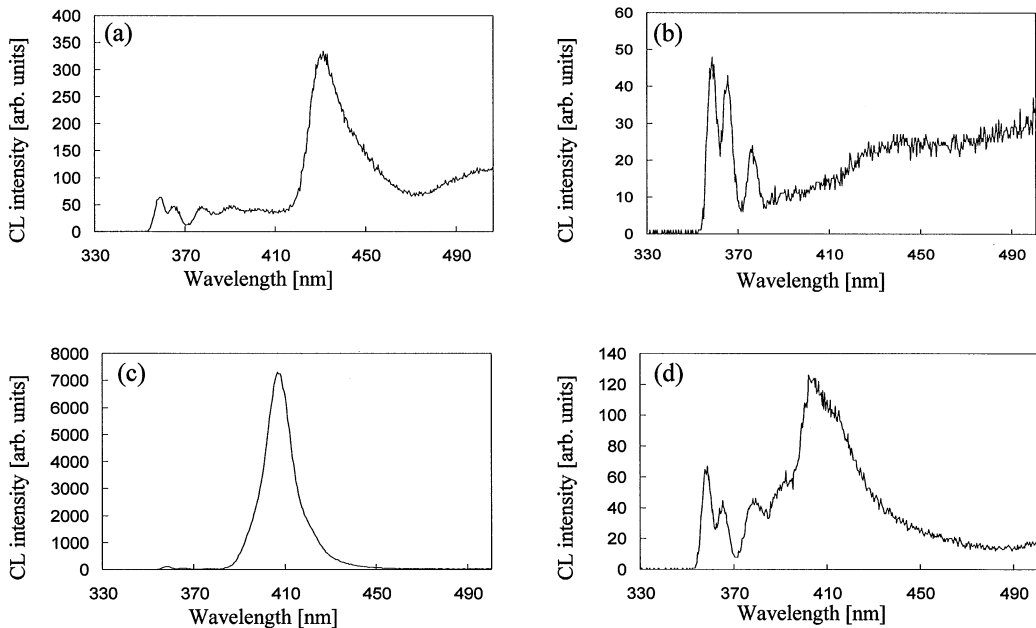


Fig. 4. CL spectra of (a)  $\text{In}_{\text{high}}$  QW ( $d_w = 50 \text{ \AA}$ ), (b)  $\text{In}_{\text{high}}$  QW ( $d_w = 100 \text{ \AA}$ ), (c)  $\text{In}_{\text{low}}$  QW ( $d_w = 40 \text{ \AA}$ ), and (d)  $\text{In}_{\text{low}}$  QW ( $d_w = 80 \text{ \AA}$ ).

The  $\text{In}_{\text{high}}$  QW ( $d_w = 50 \text{ \AA}$ ) (Fig. 4a) and  $\text{In}_{\text{low}}$  QW ( $d_w = 80 \text{ \AA}$ ) (Fig. 4d) show InGaN emission peak at 431 and 406 nm, respectively; however the intensity of both InGaN peaks is less than 5% of the peak intensity of  $\text{In}_{\text{low}}$  QW ( $d_w = 40 \text{ \AA}$ ). There are two possible causes for the decrease in the InGaN peak intensity. One is structural defects in GaN cap layer. In the  $\text{In}_{\text{high}}$  QW ( $d_w = 50 \text{ \AA}$ ), stacking faults associated with dislocations which originate at the InGaN/GaN interfaces are observed. The defects originating at the interfaces probably cause nonradiative recombination centers and decrease the luminescence efficiency. The other is In segregation. There are several reports showing that the In segregation induces the formation of In-rich quantum dot structures which help suppress the nonradiative recombination and increase the luminescence efficiency [7–10]. In our sample, the nonuniform strain contrast is observed only in thin (40–50  $\text{\AA}$ ) InGaN QW. If this strain contrast is caused by In segregation, the decrease in InGaN emission intensity in the  $\text{In}_{\text{low}}$  QW ( $d_w = 80 \text{ \AA}$ ) for which nonuniform strain contrast was not obvious can be explained by the disappearance of In segregation.

#### 4. Conclusions

The effect of In composition on the surface morphology of InGaN layers and the formation of structural defects in GaN cap layers of QWs was observed. Structural defects in the GaN cap layer reduce the intensity of InGaN emission peak in the QWs. The reduction of In composition to 16% resulted in the smooth surface morphology of InGaN layer and the suppression of structural defects originating at the interfaces.  $\text{In}_{0.16}\text{Ga}_{0.84}\text{N}$  40  $\text{\AA}$  QW with less structural defects in cap layer showed very intense and sharp InGaN emission peak in CL spectrum. HR-TEM image of this sample shows nonuniform strain contrast along InGaN/GaN interfaces, which may indicate In segregation in the InGaN layer. As the thickness of InGaN layer was increased to 80  $\text{\AA}$ , the contrast nonuniformity became less obvious and InGaN emission peak intensity decreased significantly. The mechanism to explain the dependence of In segregation on InGaN layer thickness is currently under investigation. These results indicate that structural defects in InGaN layer, structural defects originating at the InGaN/GaN interfaces and In segregation affect

the intensity of InGaN optical emission in InGaN/GaN QW structures. High efficiency QWs were only grown in this study when the QW growth temperature was as high as 775°C and the layer thickness kept as small as 40 Å.

### Acknowledgements

The authors would like to thank Mr. Saitou in Philips Japan, Ltd. for X-ray measurements. The authors gratefully acknowledge the support of the Office of Naval Research and DARPA through the National Center for Integrated Photonic Technology (NCIPT) and the GaN University Consortium at UCSB.

### References

- [1] S. Nakamura, M. Senoh, N. Iwasa, S. Nagahama, *Jpn. J. Appl. Phys. (Part 1)* 34 (1995) L797.
- [2] S. Nakamura, M. Senoh, S. Nagahama, N. Iwasa, T. Yamada, T. Matsushita, H. Kiyoku, Y. Sugimoto, *Appl. Phys. Lett.* 68 (1996) 3269.
- [3] S. Keller, B.P. Keller, D. Kapolnek, U.K. Mishra, S.P. DenBaars, I.K. Shmagin, R.M. Kolbas, S. Krishnankutty, *J. Crystal Growth* 170 (1997) 349.
- [4] F. Scholz, V. Harle, F. Steuber, H. Bolay, A. Dornen, B. Kaufmann, V. Syganow, A. Hangleiter, *J. Crystal Growth* 170 (1997) 321.
- [5] C.-K. Sun, T.-L. Chiu, S. Keller, G. Wang, M.S. Minsky, S.P. DenBaars, J.E. Bowers, *Appl. Phys. Lett.* 71 (1997) 425.
- [6] F. Scholz, V. Harle, H. Bolay, F. Steuber, B. Kaufmann, G. Reyher, A. Dornen, O. Gfroerer, S.J. Im, A. Hangleiter, *Solid State Electron.* 41 (1997) 141.
- [7] Y. Kawakami, Y. Narukawa, K. Sawada, S. Saijyo, S. Fujita, S. Nakamura, *Mater. Sci. and Eng. B* 50 (1997) 256.
- [8] S. Chichibu, T. Azuhata, T. Sota, S. Nakamura, *Appl. Phys. Lett.* 69 (1996) 4188.
- [9] S. Chichibu, K. Wada, S. Nakamura, *Appl. Phys. Lett.* 71 (1997) 2346.
- [10] H. Lakner, Q. Liu, G. Brockt, A. Radefeld, A. Meinert, F. Scholz, *Mater. Sci. Eng. B* 51 (1998) 44.
- [11] J.T. Kobayashi, N.P. Kobayashi, P.D. Dapkus, X. Zhang, D.H. Rich, *Mater. Res. Soc. Symp. Proc.* 468 (1997) 187.
- [12] J.T. Kobayashi, N.P. Kobayashi, P.D. Dapkus, *J. Electron. Matter.* 26 (1997) 1114.
- [13] J.T. Kobayashi, N.P. Kobayashi, P.D. Dapkus, Presented at American Physical Society 1998 March Meeting, Los Angeles, CA, 1998, to be published.